Multipole analysis of light scattering by arbitrary-shaped nanoparticles on a plane surface

Andrey B. Evlyukhin,[1,*] Carsten Reinhardt,[1] Egor Evlyukhin,[2] and Boris N. Chichkov[1]

[1]*Laser Zentrum Hannover e.V., Hollerithallee 8, D-30419 Hannover, Germany*
[2]*Laboratoire de Physique des Lasers-LPL, CNRS UMR 7538, Institut Galilée, Université Paris 13, 93430 Villetaneuse, France*
**Corresponding author: a.b.evlyukhin@daad-alumni.de*

Received July 9, 2013; revised August 13, 2013; accepted August 13, 2013; posted August 13, 2013 (Doc. ID 193588); published September 4, 2013

A theoretical approach, based on the discrete dipole approximation, for multipole analysis of light scattering by arbitrary-shaped nanoparticles located near or on a plane surface is presented. The obtained equations include the first multipoles up to the magnetic quadrupole and electric octupole moments. It is discussed how the suggested approach can be applied to the problem of multipole scattering of surface plasmon polaritons. As an example, the theoretical framework is used for investigation of light scattering by cylindrical Si nanoparticles located on different dielectric substrates, manifesting resonant interaction of these particles with light.

OCIS codes: (290.0290) Scattering; (240.0240) Optics at surfaces; (300.0300) Spectroscopy.
http://dx.doi.org/10.1364/JOSAB.30.002589

1. INTRODUCTION

Resonant optical responses of metal nanoparticles, due to the excitation of localized surface plasmons [1,2], and of dielectric nanoparticles with high refractive indices, due to Mie resonances [3,4], continue to attract considerable attention because of their practical applications [5–11] for nano-optical devices. Recently, it has been demonstrated experimentally that spherical silicon nanoparticles with diameters in the range of 100–200 nm have multipole Mie resonances in the visible spectral range [10,11]. It is well known that the spectral positions and quality factors of these resonances depend on the nanoparticles' size, shape, and environmental conditions, which can be used to control and tune the nanoparticle optical response. In general, the theoretical treatment is a complex problem with many independent parameters that can only be solved numerically. For the special case of nanoparticles with spherical shape located in a homogeneous medium, the analytical Mie theory can be applied for the calculation of extinction and scattering of plane electromagnetic waves. One of the main advantages of the Mie theory is the possibility to keep track of different multipole modes in the optical response of spherical nanoparticles [12,13].

A corresponding multipole analysis would also be strongly needed in studies of more complex systems with arbitrary-shaped nanoparticles located in inhomogeneous environments and irradiated by arbitrary light pulses to theoretically describe such effects as optical trapping, binding of nanoparticles [14–17], electromagnetic levitation [18,19], Fano resonances in the nanoparticle structures [5,20,21], field enhancement in nanoantennas [6,22–24], and field propagation in metamaterials [25,26]. The electromagnetic fields in those complex systems can be calculated using different numerical techniques, for example, the T-matrix approach, the multiple multipole method, the finite-difference time-domain procedure, and others [27–32]. For the case of light or surface-plasmon-polariton (SPP) scattering from nanoparticles of arbitrary shape, each of the numerical methods provides accurate results of the total field around the structure. However, the origin and contribution of the different multipole moments involved in the scattering processes demand additional nontrivial treatments.

Recently, we have suggested a theoretical approach [33] for analysis of multipole moments in the extinction and scattering spectra of nonspherical, arbitrary-shaped nanoparticles located in a homogeneous medium and irradiated by a plane light wave. This method, based on the discrete dipole approximation (DDA) [34–36], allows obtaining *a priori* information of multipole contributions to a scattering process simply from the distribution of dipoles in a structure. Since the scattering process can be decomposed into the contributing multipoles and each multipole along with its relative strength after excitation by an external light wave can be calculated separately, the method was called the decomposed discrete dipole approximation (DDDA). However, this method was up to now restricted to particles embedded in a homogeneous surrounding.

In this article, the DDDA is generalized to arbitrary-shaped nanoparticles located on or near a plane surface and irradiated by an arbitrary light wave. The excitation of different multipole moments now takes into account the influence of the surface, and the individual multipole contributions to the scattering of light or SPPs are calculated. The theoretical model is mainly focused on the first multipole moments, but detailed considerations of magnetic quadrupole and electric octupole moments are also included. Since the material of the plane surface can be arbitrary, additionally, multipole scattering of SPPs by nanoparticles located on a metal surface is discussed. Our method can further be used with the numerical Green's tensor approach in investigations of light scattering

[29]. The developed approach is illustrated using as an example resonant light scattering by cylindrical Si nanoparticles located on dielectric substrates. Angular distributions of light radiated by point multipole sources located close to dielectric or metal plane surfaces can be studied using this method.

2. GENERAL APPROACH

The optional response of nonmagnetic nanoparticles is characterized by the electric current density $\mathbf{j}_{\text{in}}$ and polarization $\mathbf{P}_{\text{in}}$ induced by external electromagnetic fields. In the case of monochromatic fields, these values are connected by $\mathbf{j}_{\text{in}} = -i\omega\mathbf{P}_{\text{in}}$. Here and in the following, we consider monochromatic fields with the time dependence defined by $\exp(-i\omega t)$, where ω is the angular frequency, and we use $\mathbf{P}_{\text{in}} \equiv \mathbf{P}$, taking into account that the optical properties of a scattering particle are characterized by its relative dielectric permittivity ε_p. The relative magnetic permeability μ of the particle is considered as $\mu = 1$, so that $\mu_0\mu = \mu_0$, where μ_0 is the vacuum permeability.

Applying the Poynting theorem [37] to the problem of electromagnetic scattering in a nonabsorbing nonmagnetic linear medium, the time-averaged extinction (scattering+absorption) power P_{ext} can be calculated by [34,38]

$$P_{\text{ext}} = \frac{\omega}{2}\,\text{Im}\int_{V_s}\mathbf{E}_0^*(\mathbf{r})\cdot\mathbf{P}(\mathbf{r})\text{d}\mathbf{r}, \tag{1}$$

where V_s is the volume of the scattering object, and $\mathbf{E}_0(\mathbf{r})$ is the electric field of the incident (external) electromagnetic waves (the field that we would have if the scattering object was not there).

The scattered electric field in the far-field (FF) zone is determined according to [37,39]

$$\mathbf{E}(\mathbf{r}) = \omega^2\mu_0\int_{V_s}\hat{G}^{\text{FF}}(\mathbf{r},\mathbf{r}')\mathbf{P}(\mathbf{r}')\text{d}\mathbf{r}', \tag{2}$$

where $\hat{G}^{\text{FF}}(\mathbf{r},\mathbf{r}')$ is the FF approximation of the Green's tensor for the system without the scattering object [37]. Thus, for the multipole decomposition of the extinction power and the scattered field, it is sufficient to have a multipole decomposition of the induced polarization. When $\hat{G}^{\text{FF}}(\mathbf{r},\mathbf{r}')$ is replaced by the total Green's tensor $\hat{G}(\mathbf{r},\mathbf{r}')$, Eq. (2) determines the electric field in all wave zones around the scatterer.

A. Multipole Presentation of Induced Polarization

In order to obtain the multipole decomposition of the polarization, we use

$$\mathbf{P}(\mathbf{r}) = \int\mathbf{P}(\mathbf{r}')\delta(\mathbf{r}-\mathbf{r}')\text{d}\mathbf{r}', \tag{3}$$

and then expand the Dirac delta function $\delta(\mathbf{r}-\mathbf{r}')$ in a Taylor series [40] around a point $\mathbf{r}_0$ with respect to $\mathbf{r}'$ (it is convenient to choose the point $\mathbf{r}_0$ at the scatterer's center of mass [33]):

$$\delta(\mathbf{r}-\mathbf{r}_0-\Delta\mathbf{r}) \simeq \delta(\mathbf{r}-\mathbf{r}_0) - (\Delta\mathbf{r}\cdot\nabla)\delta(\mathbf{r}-\mathbf{r}_0) + \frac{1}{2}(\Delta\mathbf{r}\cdot\nabla)^2\delta(\mathbf{r}-\mathbf{r}_0) - \cdots \tag{4}$$

where $\Delta\mathbf{r} = \mathbf{r}' - \mathbf{r}_0$, and ∇ is the gradient operator with respect to $\mathbf{r}$. Inserting Eq. (4) in Eq. (3) and using the definitions of the corresponding multipole moments, we can write (see Appendix A)

$$\mathbf{P}(\mathbf{r}) \simeq \mathbf{p}\delta(\mathbf{r}-\mathbf{r}_0) - \frac{1}{6}\hat{Q}\nabla\delta(\mathbf{r}-\mathbf{r}_0) + \frac{i}{\omega}[\nabla\times\mathbf{m}\delta(\mathbf{r}-\mathbf{r}_0)] + \frac{1}{6}\hat{O}(\nabla\nabla\delta(\mathbf{r}-\mathbf{r}_0)) - \frac{i}{2\omega}[\nabla\times\hat{M}\nabla\delta(\mathbf{r}-\mathbf{r}_0)], \tag{5}$$

where

$$\mathbf{p} = \int\mathbf{P}(\mathbf{r}')\text{d}\mathbf{r}' \tag{6}$$

is the electric dipole moment, and

$$\hat{Q} \equiv \hat{Q}(\mathbf{r}_0) = 3\int(\Delta\mathbf{r}\mathbf{P}(\mathbf{r}') + \mathbf{P}(\mathbf{r}')\Delta\mathbf{r})\text{d}\mathbf{r}', \tag{7}$$

$$\mathbf{m} \equiv \mathbf{m}(\mathbf{r}_0) = -\frac{i\omega}{2}\int[\Delta\mathbf{r}\times\mathbf{P}(\mathbf{r}')]\text{d}\mathbf{r}', \tag{8}$$

$$\hat{O} \equiv \hat{O}(\mathbf{r}_0) = -\int\Delta\mathbf{r}\Delta\mathbf{r}\Delta\mathbf{r}(\nabla\cdot\mathbf{P}(\mathbf{r}'))\text{d}\mathbf{r}', \tag{9}$$

$$\hat{M} \equiv \hat{M}(\mathbf{r}_0) = -\frac{2i\omega}{3}\int[\Delta\mathbf{r}\times\mathbf{P}(\mathbf{r}')]\Delta\mathbf{r}\text{d}\mathbf{r}' \tag{10}$$

are the electric quadrupole tensor, the magnetic dipole moment, the tensor of the electric octupole moment, and the tensor of the magnetic quadrupole moment, respectively, at the point $\mathbf{r}_0$. Here $\nabla\nabla$, $\Delta\mathbf{r}\mathbf{P}$, and $\Delta\mathbf{r}\Delta\mathbf{r}\Delta\mathbf{r}$ represent the dyadic products between corresponding vectors. We consider the electric quadrupole tensor as totally symmetric and not traceless. Note that the electric quadrupole contribution into the extinction and scattering cross sections (SCSs) is independent of the electric quadrupole term presentation [41]. The tensor $\hat{M}$ is traceless and not symmetric, whereas $\hat{O}$ is totally symmetric and not traceless [12]. Note that if we chose $\hat{M}$ and $\hat{O}$ in the total symmetrical and traceless tensor presentations, the toroid-dipole term in the multipole decomposition would appear [12]. For atomic systems, the electric and magnetic multipole moments can be found in [42].

B. Multipole Decomposition of Extinction

Inserting Eq. (5) in Eq. (1) and after integration one obtains the multipole presentation of the extinction power up to the magnetic quadrupole and electric octupole terms

$$P_{\text{ext}} \simeq P_{\text{ext}}^p + P_{\text{ext}}^m + P_{\text{ext}}^Q + P_{\text{ext}}^M + P_{\text{ext}}^O. \tag{11}$$

Dividing the extinction power by the radiation flux of the incident (external) wave P_{in}, we obtain the extinction cross section (ECS)

$$\sigma_{\text{ext}} = \frac{P_{\text{ext}}}{P_{\text{in}}} \simeq \sigma_{\text{ext}}^p + \sigma_{\text{ext}}^m + \sigma_{\text{ext}}^Q + \sigma_{\text{ext}}^M + \sigma_{\text{ext}}^O, \tag{12}$$

where the electric dipole ECS

$$\sigma_{\text{ext}}^p = \frac{P_{\text{ext}}^p}{P_{\text{in}}} = \frac{\omega}{2P_{\text{in}}}\,\text{Im}[\mathbf{E}_0^*(\mathbf{r}_0)\cdot\mathbf{p}], \tag{13}$$

the magnetic dipole ECS

$$\sigma_{\text{ext}}^{m} = \frac{P_{\text{ext}}^{m}}{P_{\text{in}}} = \frac{\omega}{2P_{\text{in}}} \text{Im}[\mu_0 \mathbf{H}_0^*(\mathbf{r}_0) \cdot \mathbf{m}(\mathbf{r}_0)], \quad (14)$$

the electric quadrupole ECS

$$\sigma_{\text{ext}}^{Q} = \frac{P_{\text{ext}}^{Q}}{P_{\text{in}}} = \frac{\omega}{24P_{\text{in}}} \text{Im}[\{\nabla \mathbf{E}_0^*(\mathbf{r}_0) + (\nabla \mathbf{E}_0^*(\mathbf{r}_0))^T\} : \hat{Q}(\mathbf{r}_0)], \quad (15)$$

the magnetic quadrupole ECS

$$\sigma_{\text{ext}}^{M} = \frac{P_{\text{ext}}^{M}}{P_{\text{in}}} = \frac{\omega}{4P_{\text{in}}} \text{Im}(\mu_0 [\nabla \mathbf{H}_0^*(\mathbf{r}_0)]^T : \hat{M}(\mathbf{r}_0)), \quad (16)$$

and the electric octupole ECS

$$\sigma_{\text{ext}}^{O} = \frac{P_{\text{ext}}^{O}}{P_{\text{in}}} = \frac{\omega}{12P_{\text{in}}} \text{Im} \sum_{\beta\gamma\tau} O_{\beta\gamma\tau}(\mathbf{r}_0) \frac{\partial^2}{\partial\gamma\partial\tau} E_{0\beta}^*(\mathbf{r}_0). \quad (17)$$

Here $\mathbf{H}_0(\mathbf{r}_0)$ is the magnetic field of the incident wave at the point $\mathbf{r}_0$, $\alpha = x, y, z$; $\beta = x, y, z$; $\gamma = x, y, z$, T denotes the transpose operation, the sign : denotes the double scalar product of dyads [33], and the sum in Eq. (17) denotes summations over all coordinates

$$\sum_{\beta\gamma\tau} \equiv \sum_{\beta} \sum_{\gamma} \sum_{\tau}.$$

The values $\nabla \mathbf{E}_0(\mathbf{r}_0)$ and $\nabla \mathbf{H}_0(\mathbf{r}_0)$ are the gradients of electric and magnetic fields, respectively, at the point $\mathbf{r}_0$ [33,43].

C. Multipole Decomposition of Scattered Fields

A multipole decomposition of the scattered electric field into the FF zone can be obtained by inserting Eq. (5) in Eq. (2). The integration is easily carried out in the FF approximation when the Green's tensor $\hat{G}^{\text{FF}}$ or its parts can be presented in a special form:

$$\hat{G}^{\text{FF}}(\mathbf{r}, \mathbf{r}') = \hat{g}(\mathbf{r}) e^{(\mathbf{N}\cdot\mathbf{r}')}, \quad (18)$$

where the tensor $\hat{g}(\mathbf{r})$ is independent of the point $\mathbf{r}'$, and $\mathbf{N}$ is a vector that also does not depend on the scatterer position $\mathbf{r}'$. Using Eq. (18), the scattered electric fields can be presented as

$$\mathbf{E}(\mathbf{r}) = \frac{k_0^2}{\varepsilon_0} \hat{g}(\mathbf{r}) \int e^{(\mathbf{N}\cdot\mathbf{r}')} \Big\{ \mathbf{p}\delta(\mathbf{r}' - \mathbf{r}_0) - \frac{1}{6}\hat{Q}\nabla\delta(\mathbf{r}' - \mathbf{r}_0) + \frac{i}{\omega}[\nabla \times \mathbf{m}\delta(\mathbf{r}' - \mathbf{r}_0)] + \frac{1}{6}\hat{O}(\nabla\nabla\delta(\mathbf{r}' - \mathbf{r}_0)) - \frac{i}{2\omega}[\nabla \times \hat{M}\nabla\delta(\mathbf{r}' - \mathbf{r}_0)] \Big\} d\mathbf{r}', \quad (19)$$

where we used the identity $\omega^2\mu_0 = k_0^2/\varepsilon_0$ (k_0 is the wave number in vacuum and ε_0 is the vacuum dielectric constant).

After the integration, the scattered electric field is obtained from Eq. (19) by replacing every ∇ with the vector $-\mathbf{N}$ and $\mathbf{r}'$ by $\mathbf{r}_0$:

$$\mathbf{E}(\mathbf{r}) = \frac{k_0^2}{\varepsilon_0} \hat{g}(\mathbf{r}) e^{(\mathbf{N}\cdot\mathbf{r}_0)} \Big\{ \mathbf{p} + \frac{1}{6}\hat{Q}\mathbf{N} - \frac{i}{\omega}[\mathbf{N} \times \mathbf{m}] + \frac{1}{6}\hat{O}(\mathbf{NN}) - \frac{i}{2\omega}[\mathbf{N} \times \hat{M}\mathbf{N}] \Big\}. \quad (20)$$

From Eq. (20), one can derive a *useful* general rule: expressions for the electric fields radiated or scattered into the FF zone by electric (magnetic) multipole moments higher than the electric (magnetic) dipole can be easily obtained on the basis of expressions for the electric (magnetic) dipole performing certain replacements. For example, if in the expression for the electric field of an electric dipole one substitutes the dipole moment p by $(1/6)\hat{Q}\mathbf{N}$ or $(1/6)\hat{O}(\mathbf{NN})$, one obtains the electric field radiated by the electric quadrupole or electric octupole moments, respectively. The electric field of the magnetic quadrupole moment is obtained from the electric field of the magnetic dipole substituting m by $(1/2)\hat{M}\mathbf{N}$.

If the scatterer is located in a homogeneous medium with relative dielectric constant ε_d, the FF approximation of the Green's tensor has the following form [44]:

$$\hat{G}^{\text{FF}}(\mathbf{r}, \mathbf{r}') = \frac{e^{ik_d r}}{4\pi r}(\hat{U} - \mathbf{nn}) e^{-ik_d(\mathbf{n}\cdot\mathbf{r}')}, \quad (21)$$

where $k_d = \omega/v_d \equiv k_0\sqrt{\varepsilon_d}$ is the light wave number in medium with ε_d (v_d is the corresponding phase speed of light), $\hat{U}$ is the 3×3 unit tensor, and n is the unit vector directed along r. Comparing Eqs. (18) and (21), one can see that $\mathbf{N} \equiv -ik_d\mathbf{n}$ and the scattered electric field can be obtained from Eq. (20) using Eq. (21) [33]:

$$\mathbf{E}(\mathbf{r}) \simeq \frac{k_0^2 e^{ik_d(r - \mathbf{n}\cdot\mathbf{r}_0)}}{4\pi\varepsilon_0 r} \Big([\mathbf{n} \times [\mathbf{p} \times \mathbf{n}]] + \frac{1}{v_d}[\mathbf{m} \times \mathbf{n}] + \frac{ik_d}{6}[\mathbf{n} \times [\mathbf{n} \times \hat{Q}\mathbf{n}]] + \frac{ik_d}{2v_d}[\mathbf{n} \times (\hat{M}\mathbf{n})] + \frac{k_d^2}{6}[\mathbf{n} \times [\mathbf{n} \times \hat{O}(\mathbf{nn})]] \Big). \quad (22)$$

Here, we used the equality

$$(\hat{U} - \mathbf{nn})\mathbf{b} = [\mathbf{n} \times [\mathbf{b} \times \mathbf{n}]]$$

for an arbitrary vector $\mathbf{b}$. If the origin of the Cartesian coordinate system is chosen at the point $\mathbf{r}_0$ (location of multipoles), the factor $\exp(-ik_d\mathbf{n} \cdot \mathbf{r}_0)$ disappears in Eq. (22). The scattered magnetic field $\mathbf{H}$ is obtained from the electric field using Maxwell equation $[\nabla \times \mathbf{E}] = i\omega\mu_0\mathbf{H}$.

The extinction power (1) and scattered fields (2) do not depend on the point $\mathbf{r}_0$, whereas the high-order multipole moments can be strongly affected by the choice of this point. In general, it is necessary to take into account all terms in the multipole expansions. However, if the sizes of scattering nanoparticles are smaller than the space variations of the incident electromagnetic fields and the position of the point $\mathbf{r}_0$ is chosen in the region occupied by the scatterer (for example, at the scatterer center of mass), the multipole expansion converges fast and only the first several terms need to be taken into account.

3. PARTICLE ON A PLANE SURFACE

The theoretical approach presented above can now be applied to the case in which the scatterer is located near or on the surface of a solid substrate.

A. Dielectric Substrate

We consider an arbitrary-shaped particle placed near a dielectric or metallic substrate (with the relative permittivity ε_s) in a medium with the relative dielectric constant ε_d (Fig. 1). The imaginary parts of ε_d and ε_s are assumed to be negligibly small. The particle is irradiated by an external

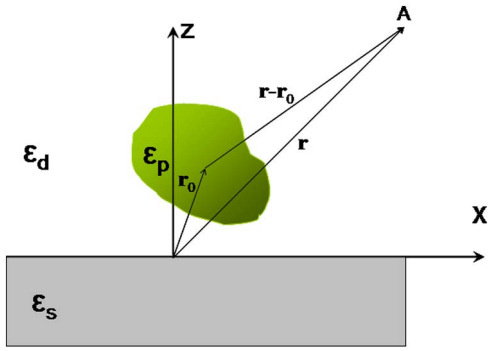

Fig. 1. Schematic representation of a scattering system and the chosen Cartesian coordinate system. $\mathbf{r}_0$ is the point where multipole moments are located; A is the observation point.

electromagnetic wave. We distinguish two different radiation cases: (i) the particle is irradiated from the side of the medium with ε_d; (ii) the particle is irradiated from the side of the substrate. Assuming that we know the induced polarization $\mathbf{P}$ of the scattering particle, the extinction power can be calculated using Eq. (1). In case (i), the external electric field $\mathbf{E}_0$ is a superposition of the incident and reflected waves, which would be in the system without the particle. In the second case (ii), $\mathbf{E}_0$ is the electric field of the transmitted wave, which would be in the system without the particle (scatterer). In both cases the multipole decomposition of the extinction powers or of the ECSs up to the magnetic quadrupole and the electric octupole contributions is determined by Eqs. (11)–(17) with the corresponding electric and magnetic fields and their spatial derivatives.

In the framework of the Green's tensor formalism, the scattered electric field above the substrate in the FF region is determined by

$$\mathbf{E}_a(\mathbf{r}) = \omega^2\mu_0 \int_{V_s} \{\hat{G}_0^{\mathrm{FF}}(\mathbf{r},\mathbf{r}') + \hat{G}_R^{\mathrm{FF}}(\mathbf{r},\mathbf{r}')\}\mathbf{P}(\mathbf{r}')\mathrm{d}\mathbf{r}', \tag{23}$$

and in the substrate by the expression

$$\mathbf{E}_t(\mathbf{r}) = \omega^2\mu_0 \int_{V_s} \hat{G}_T^{\mathrm{FF}}(\mathbf{r},\mathbf{r}')\mathbf{P}(\mathbf{r}')\mathrm{d}\mathbf{r}', \tag{24}$$

where $\hat{G}_0^{\mathrm{FF}}$ is the FF approximation of the Green's tensor in a homogeneous medium with ε_d, and the tensors $\hat{G}_R^{\mathrm{FF}}$ and $\hat{G}_T^{\mathrm{FF}}$ describe reflection from and transmission through the substrate surface, respectively, in the FF region. We choose the Cartesian coordinate system as it is shown in Fig. 1. In the FF region, where $|\mathbf{r}-\mathbf{r}'| \gg \lambda$ for any $\mathbf{r}'$ from the region occupied by the particle (λ is the radiation wavelength), one can write [37,39]

$$\hat{G}_0^{\mathrm{FF}}(\mathbf{r},\mathbf{r}') = \frac{e^{ik_d r}}{4\pi r}(\hat{U} - \mathbf{nn})e^{-ik_d(\mathbf{n}\cdot\mathbf{r}')}, \tag{25}$$

$$\hat{G}_R^{\mathrm{FF}}(\mathbf{r},\mathbf{r}') = \frac{e^{ik_d r}}{4\pi r}\hat{R}(\mathbf{r})e^{-ik_d(\tilde{\mathbf{n}}\cdot\mathbf{r}')}, \tag{26}$$

$$\hat{G}_T^{\mathrm{FF}}(\mathbf{r},\mathbf{r}') = \frac{e^{ik_S r}}{4\pi r}\hat{T}(\mathbf{r})e^{-ik_d(\tilde{\tilde{\mathbf{n}}}\cdot\mathbf{r}')}, \tag{27}$$

where $k_S = k_0\sqrt{\varepsilon_s}$, $\mathbf{n} = \mathbf{r}/r$, $\tilde{\mathbf{n}} = \tilde{\mathbf{r}}/r$, $\tilde{\tilde{\mathbf{n}}} = \tilde{\tilde{\mathbf{r}}}/r$, $\mathbf{r} = (x,y,z)$, $\tilde{\mathbf{r}} = (x,y,-z)$, $\tilde{\tilde{\mathbf{r}}} = (x,y,-\sqrt{r^2 - \varepsilon_s\rho^2/\varepsilon_d})$, and $\rho = \sqrt{x^2+y^2}$, and the tensors $\hat{R}(\mathbf{r})$ and $\hat{T}(\mathbf{r})$ depend only on the position of the observation point $\mathbf{r}$ and can be obtained from Eqs. (D4)–(D7) in [37]. Note that in [37], there is a general FF approximation (asymptotic) of the Green's tensor for a multilayered medium. This approximation can be easily transformed for a one-interface system, which is considered in our paper. Particularly, the tensor $\hat{R}(\mathbf{r})$ for the one-interface system can be obtained from expressions (6) and (7) in [39].

The tensors (25)–(27) have the same structure as Eq. (18). Therefore, the abovedeveloped approach for multipole decomposition of scattered fields can be applied [Eq. (20)]. As a result, one obtains the scattered electric field above the substrate

$$\mathbf{E}_a(\mathbf{r}) = \mathbf{E}_d(\mathbf{r}) + \mathbf{E}_r(\mathbf{r}), \tag{28}$$

where $\mathbf{E}_d(\mathbf{r})$ is the electric field of the wave directly scattered in the observation point $\mathbf{r}$ [Eq. (22)], and $\mathbf{E}_r$ is the electric field of the scattered wave reflected from the substrate surface

$$\mathbf{E}_r(\mathbf{r}) \simeq \frac{k_0^2 e^{ik_d(r-\tilde{\mathbf{n}}\cdot\mathbf{r}_0))}}{4\pi\varepsilon_0 r}\hat{R}(\mathbf{r})\Big\{\mathbf{p} - \frac{ik_d}{6}\hat{Q}\tilde{n} - \frac{k_d}{\omega}[\tilde{\mathbf{n}}\times\mathbf{m}] - \frac{k_d^2}{6}\hat{O}(\tilde{\mathbf{n}}\,\tilde{\mathbf{n}}) + \frac{ik_d^2}{2\omega}[\tilde{\mathbf{n}}\times\hat{M}\,\tilde{\mathbf{n}}]\Big\}. \tag{29}$$

In the substrate the electric field of the scattered wave is determined by the expression (in FF approximation)

$$\mathbf{E}_t(\mathbf{r}) \simeq \frac{k_0^2 e^{ik_S r - ik_d\tilde{\tilde{\mathbf{n}}}\cdot\mathbf{r}_0}}{4\pi\varepsilon_0 r}\hat{T}(\mathbf{r})\Big\{\mathbf{p} - \frac{ik_d}{6}\hat{Q}\tilde{\tilde{\mathbf{n}}} - \frac{k_d}{\omega}[\tilde{\tilde{\mathbf{n}}}\times\mathbf{m}] - \frac{k_d^2}{6}\hat{O}(\tilde{\tilde{\mathbf{n}}}\,\tilde{\tilde{\mathbf{n}}}) + \frac{ik_d^2}{2\omega}[\tilde{\tilde{\mathbf{n}}}\times\hat{M}\,\tilde{\tilde{\mathbf{n}}}]\Big\}. \tag{30}$$

The rule formulated after Eq. (20) for the determination of multipole electric fields is applied here for $\mathbf{N} \equiv -ik_d\tilde{\mathbf{n}}$ (reflected fields) and $\mathbf{N} \equiv -ik_d\tilde{\tilde{\mathbf{n}}}$ (transmitted fields). The spherical coordinate presentation (in the FF zone) of the electric field radiated by an electric dipole located above a multilayered structure can be found in [37]. These expressions can be applied for the one-interface system by using corresponding reflection and transmission coefficients. The spherical coordinate presentations of electric fields radiated by electric and magnetic dipoles located near a substrate surface are given in Appendix B.

Using the electric fields of scattered waves it is possible to calculate angular distributions of the scattered (radiated) powers above and into the substrate. The FF scattered (radiated) power $\mathrm{d}P$ into the solid angle $\mathrm{d}\Omega = \sin\theta\mathrm{d}\varphi\mathrm{d}\theta$ above the substrate is determined by the expression

$$\mathrm{d}P = \frac{1}{2}\sqrt{\frac{\varepsilon_0\varepsilon_d}{\mu_0}}|\mathbf{E}_a|^2 r^2 \mathrm{d}\Omega, \tag{31}$$

where $\mathbf{E}_a \simeq \mathbf{E}^p + \mathbf{E}^m + \mathbf{E}^Q + \mathbf{E}^M + \mathbf{E}^O$. The FF scattered (radiated) power $\mathrm{d}P$ into the solid angle $\mathrm{d}\Omega = \sin\theta\mathrm{d}\varphi\mathrm{d}\theta$ below the substrate surface is determined by Eq. (31), replacing ε_d by ε_s and $\mathbf{E}_a$ by $\mathbf{E}_t$.

An SCS into a finite-size solid angle $\Delta\Omega$ is obtained by integrating dP over this angle and normalizing the obtained result on the radiation flux of the incident wave P_{in}. Multipole

decomposition of the scattered fields allows understanding of the interference effects between the fields generated by different multipoles.

B. Nontransparent Substrate

For nontransparent substrates, only reflection can be measured directly. In these conditions it is more consistent to speak about the SCS. The power of scattered light by a nanoparticle located on or near a nontransparent substrate (metals, semiconductors) can be calculated using Eq. (31). For example, the light power P_b scattered into the semi-space above the substrate surface (total back scattering) can be calculated from

$$P_b = \frac{1}{2}\sqrt{\frac{\varepsilon_0\varepsilon_d}{\mu_0}}\int_0^{\pi/2}\int_0^{2\pi}|\mathbf{E}_a|^2 r^2 \mathrm{d}\sin\theta \mathrm{d}\theta\mathrm{d}\varphi, \tag{32}$$

where φ and θ are the azimuthal and polar angles of the spherical coordinate system, respectively. The role of different nanoparticle multipoles is estimated using multipole decomposition of the scattered electric field $\mathbf{E}_a$. The back SCS is determined as a ratio between Eq. (32) and the radiation flux of the incident (external) wave P_{in}.

C. Substrate Supporting SPP Propagation

We assume that the scattering nanoparticle is located near a metal surface supporting propagation of SPPs. This means that $-\mathrm{Re}(\varepsilon_s) > \varepsilon_d$ and $-\mathrm{Re}(\varepsilon_s) \gg \mathrm{Im}(\varepsilon_s)$. The last inequality guaranties that the SPP propagation length is larger than the SPP wavelength. In these conditions, for the sake of simplicity, we can neglect the imaginary part of ε_s for calculations of SPP power in the FF region [39].

When the nanoparticle is illuminated either by a light wave incident on the substrate or by a SPP wave propagating along the substrate surface, an additional scattering channel into SPPs propagating along the metal surface in different directions appears. The scattered electric field above the surface ($z > 0$, Fig. 1) in the FF zone ε_d is

$$\mathbf{E}_a(\mathbf{r}) = \mathbf{E}_d(\mathbf{r}) + \mathbf{E}_r(\mathbf{r}) + \mathbf{E}_{\mathrm{SPP}}(\mathbf{r}), \tag{33}$$

where the field $\mathbf{E}_d(\mathbf{r})$ is determined by Eq. (22), the reflected electric field $\mathbf{E}_r(\mathbf{r})$ is given by Eq. (29), and the SPP electric field $\mathbf{E}_{\mathrm{SPP}}(\mathbf{r})$ is [39]

$$\mathbf{E}_{\mathrm{SPP}}(\mathbf{r}) = \omega^2\mu_0\int_{V_s}\hat{G}_{\mathrm{SPP}}(\mathbf{r},\mathbf{r}')\mathbf{P}(\mathbf{r}')\mathrm{d}\mathbf{r}'. \tag{34}$$

In the FF approximation, the tensor $\hat{G}_{\mathrm{SPP}}(\mathbf{r},\mathbf{r}')$ describing the excitation and propagation of SPPs can be presented in the following form [39]:

$$\hat{G}^{\mathrm{FF}}_{\mathrm{SPP}}(\mathbf{r},\mathbf{r}') = \hat{S}_p(\mathbf{r})e^{-ik_p(\mathbf{n}_p\cdot\mathbf{r}')}, \tag{35}$$

where the tensor $\hat{S}_p(\mathbf{r})$ does not depend on the scatterer position $\mathbf{r}'$, $k_p = \sqrt{\varepsilon_s\varepsilon_d/(\varepsilon_s+\varepsilon_d)}$ is the SPP wave number, and the vector $\mathbf{n}_p = (x/\rho, y/\rho, -i\sqrt{-\varepsilon_d/\varepsilon_s})$, $\rho = \sqrt{x^2+y^2}$. Applying Eq. (20) to the SPP scattered waves with $\mathbf{N} \equiv -ik_p\mathbf{n}_p$, one obtains multipole decomposition of the SPP electric field radiated by the scatterer

$$\mathbf{E}_{\mathrm{SPP}}(\mathbf{r}) \simeq \frac{k_0^2 e^{-ik_p\mathbf{n}_p\cdot\mathbf{r}_0}}{\varepsilon_0}\hat{S}_p(\mathbf{r})\Big\{\mathbf{p} - \frac{k_p}{\omega}[\mathbf{n}_p\times\mathbf{m}] - \frac{ik_p}{6}\hat{Q}\mathbf{n}_p - \frac{k_p^2}{6}\hat{O}(\mathbf{n}_p\mathbf{n}_p) + \frac{ik_p^2}{2\omega}[\mathbf{n}_p\times\hat{M}\mathbf{n}_p]\Big\}. \tag{36}$$

Below the substrate surface ($z < 0$), the scattered electric field of SPPs is determined by Eq. (36). The tensor $\hat{S}_p$ has different components for $z > 0$ and $z < 0$, which are related by boundary conditions [39]. Expressions for the electric fields radiated by high multipole moments can be obtained from the corresponding expressions for the electric and magnetic dipoles by applying the general rule with $\mathbf{N} = -ik_p\mathbf{n}_p$. The electric and magnetic fields of the SPP waves generated by the electric and magnetic dipoles are shown in Appendix C.

In the case of SPP scattering by nanoparticles, the external incident electric field in Eq. (1) corresponds to the electric field of the incident SPP wave [39]. Multipole decomposition of the SPP extinction power (and of the ECS) is obtained using Eqs. (11)–(17). Multipole representations of the scattered fields (22), (29), (30), and (36) are independent of the illumination conditions and can be used for light and SPP scattering. In the FF zone, spatial overlap between the scattered SPP and light waves disappears and the corresponding scattered powers can be estimated separately [39].

The SPP power scattered by a scatterer located near a metal surface into an in-plane angle $[\varphi, \varphi + d\varphi]$ (the polar coordinate system as in Appendix C) is determined by the expression

$$p(\varphi)d\varphi = \sqrt{\frac{\mu_0}{\varepsilon_0}}\frac{(1-a^2)(1-a^4)}{4ak_0}|E_{\mathrm{SPP}z}|^2\rho\mathrm{d}\varphi, \tag{37}$$

where the z component of the scattered SPP electric field $E_{\mathrm{SPP}z}$ is taken in the domain above the metal surface and for $z = 0$; $a = \sqrt{-\varepsilon_d/\varepsilon_s}$. Note that the expression (37) was obtained by neglecting the imaginary part of metal permittivity ε_s. The total SPP scattered power is obtained by integrating Eq. (37) over $\varphi \in [0, 2\pi]$. Using the electric field $E_{\mathrm{SPP}z}$ as a superposition of multipole contributions (36), the importance of different multipoles in the scattered SPP power can be estimated. Normalizing the total scattered SPP power by the radiation flux of the incident wave P_{in}, we obtain the corresponding SCS.

4. MULTIPOLE MOMENTS IN DDA

For application of the multipole decomposition approach to an arbitrary-shaped scatterer, one has to (i) find the induced polarization $\mathbf{P}(\mathbf{r})$ of the scatterer, (ii) calculate its multipole moments, and (iii) define the scattered or extinction powers.

In general, the polarization $\mathbf{P}(\mathbf{r})$ can be calculated only numerically. We apply DDA for this goal. The main idea of DDA consists in the replacement of the scattering object by a cubic lattice of electric point dipoles with a polarizability of α_p. The corresponding dipole moment $\mathbf{p}_j$ induced in each lattice point j (with the radius vector $\mathbf{r}_j$) is found by solving coupled-dipole equations. For the scattering particle located near a substrate surface, these equations can be presented by [45]

$$\mathbf{p}_j = \alpha_p\mathbf{E}_0(\mathbf{r}_j) + \frac{k_0^2}{\varepsilon_0}\alpha_p\hat{G}_S(\mathbf{r}_j,\mathbf{r}_j)\mathbf{p}_j + \frac{k_0^2}{\varepsilon_0}\alpha_p\sum_{l\neq j}^{N}\hat{G}(\mathbf{r}_j,\mathbf{r}_l)\mathbf{p}_l, \tag{38}$$

where $\hat{G}(\mathbf{r}_j, \mathbf{r}_l)$ is the Green's tensor of the system without the scatterer [37], $\hat{G}_S(\mathbf{r}_j, \mathbf{r}_j)$ is the part of the total Green's tensor $\hat{G}$ taking into account the electric field scattered by the substrate surface [45], and N is the total number of point dipoles in the considered system. Detail discussion of DDA realizations and their connections with the Green's tensor approach can be found elsewhere [36]. In general, calculation of the tensor $\hat{G}_S(\mathbf{r}, \mathbf{r}')$ involves numerical integrations of the Sommerfeld-type integrals [38,45,46]. If the scatterer size is small compared to the wavelength of incident light and is located on substrate surfaces, it is possible to use a simple analytical near-field approximation of $\hat{G}_S(\mathbf{r}, \mathbf{r}')$ based on the method of images [47]. However, as will be shown in Section 5, discrepancy between the near-field approximation and the total-retardation calculation can be significant in the case of high dielectric constant substrates. Note that our multipole method can be also used in the framework of the Green's tensor approach in which the total electric field E is calculated instead of the induced polarization P, taking into account that $\mathbf{P} = \varepsilon_0(\varepsilon_p - \varepsilon_d)\mathbf{E}$.

After solution of Eqs. (38), the induced polarization $\mathbf{P}(\mathbf{r})$ of the scatterer is

$$\mathbf{P}(\mathbf{r}) = \sum_{j=1}^{N} \mathbf{p}_j \delta(\mathbf{r} - \mathbf{r}_j). \tag{39}$$

Inserting Eq. (39) into Eqs. (6)–(10), one obtains the discrete dipole representation of multipole moments up to the magnetic quadrupole and electric octupole [33]

$$\mathbf{p} = \sum_{j=1}^{N} \mathbf{p}_j; \qquad \hat{Q}(\mathbf{r}_0) = \sum_{j=1}^{N} \hat{Q}^j(\mathbf{r}_0); \qquad \mathbf{m}(\mathbf{r}_0) = \sum_{j=1}^{N} \mathbf{m}_j(\mathbf{r}_0);$$
$$\hat{M}(\mathbf{r}_0) = \sum_{j=1}^{N} \hat{M}^j(\mathbf{r}_0); \qquad \hat{O}(\mathbf{r}_0) = \sum_{j=1}^{N} \hat{O}^j(\mathbf{r}_0), \tag{40}$$

where $\mathbf{p}_j$, $\hat{Q}^j(\mathbf{r}_0)$, $\mathbf{m}_j(\mathbf{r}_0)$, $\hat{M}^j(\mathbf{r}_0)$, and $\hat{O}^j(\mathbf{r}_0)$ are the corresponding point multipole moments localized at the point $\mathbf{r}_0$ associated with the corresponding single dipole j of the scatterer [33]. One obtains

$$\hat{Q}^j(\mathbf{r}_0) = 3((\mathbf{r}_j - \mathbf{r}_0)\mathbf{p}_j + \mathbf{p}_j(\mathbf{r}_j - \mathbf{r}_0)), \tag{41}$$

$$\mathbf{m}_j(\mathbf{r}_0) = -\frac{i\omega}{2}[(\mathbf{r}_j - \mathbf{r}_0) \times \mathbf{p}_j], \tag{42}$$

$$\hat{M}^j(\mathbf{r}_0) = -\frac{i2\omega}{3}[(\mathbf{r}_j - \mathbf{r}_0) \times \mathbf{p}_j](\mathbf{r}_j - \mathbf{r}_0), \tag{43}$$

$$O^j_{\beta\beta\beta} = 3p_{j\beta}(\beta_j - \beta_0)^2,$$
$$O^j_{\beta\beta\gamma} = O^j_{\beta\gamma\beta} = O^j_{\gamma\beta\beta} = 2p_{j\beta}(\beta_j - \beta_0)(\gamma_j - \gamma_0),$$
$$O^j_{\beta\gamma\tau} = p_{j\beta}(\gamma_j - \gamma_0)(\tau_j - \tau_0) + p_{j\gamma}(\beta_j - \beta_0)(\tau_j - \tau_0)$$
$$+ p_{j\tau}(\gamma_j - \gamma_0)(\beta_j - \beta_0), \tag{44}$$

where $\beta = x, y, z$, $\gamma = x, y, z$, and $\tau = x, y, z$; moreover, $\beta \neq \gamma$, $\beta \neq \tau$, and $\tau \neq \gamma$, and the electric dipole moment $\mathbf{p}_j$ has the coordinates (p_{jx}, p_{jy}, p_{jz}). Note that the computational accuracy of the extinction and SCSs calculated in the framework of the DDDA coincides with that of DDA.

5. NUMERICAL RESULTS AND DISCUSSION

The developed approach can be used for investigations of multipole moment contributions into the resonance optical response of arbitrary-shaped nanoparticles located either in a homogeneous medium or near a substrate surface. For a demonstration, we calculate the ECS and SCS of cylindrical Si nanoparticles (the diameter and height are 150 and 75 nm, respectively) located in different environments. Compared to spherical particles, cylindrical particles more strongly interact with the substrate surface, due to a larger contact area. In contrast to metal nanoparticles, Si nanoparticles can resonantly interact with both electric and magnetic light components and can scatter light like electric and magnetic dipoles [44]. Si dielectric permittivity is taken from [48]. In our simulations we consider external light as a linear-polarized plane wave impinging normally on the substrate surface located in air. In general, due to asymmetric environment, the light scattering spectra of nanoparticles can depend on the incident direction of the external light wave.

Figure 2 demonstrates extinction spectra of Si nanoparticles located in free space and on a Si substrate. ECSs for nanoparticles located on glass and Si substrates are determined as the extinction powers normalized on the incident radiation flux. Also multipole decompositions of the ECSs are presented. There are contributions of three main multipoles (all multipoles are located at the nanoparticle center of mass): electric dipole (ED); magnetic dipole (MD); and electric quadrupole (EQ). The contributions of other high-order multipoles are negligibly small. By comparing the total ECSs in Fig. 2 (red circle curves), one can see that there is a red shift and broadening of the main resonance due to the substrate influence increasing with the growing substrate refractive index, which is consistent with the results reported recently [8]. In all cases, the ED and MD modes have resonances (maxima) in the visible spectral range. These resonances are also shifted and broadened with the increasing substrate refraction index. However, the red shift is larger for the ED resonance than that for the MD resonance. The multipole decomposition shows that the ECS resonance in Figs. 2(a) and 2(b) is composed from the two resonant contributions and that Si nanoparticles resonantly interact with both electric and magnetic components of the incident light. For the Si nanoparticle on the Si substrate [Fig. 2(c)], there is a considerable negative contribution of the EQ mode due to the substrate influence. In this case, the EQ part of the electromagnetic energy is formally returned into the incident light. In general, we should take into account that the considered multipole modes are not the eigenmodes of the system [49]. Due to the asymmetric environment, interactions between different multipole modes [50,51] can occur, leading to negative contributions of certain modes into the total ECS. However, the total ECSs are always positive for passive systems. Note that a small negative contribution of the quadrupole term into the total ECS shown in Fig. 2(a) appears as a result of discretization approximation for cylindrical nanoparticles and can be considered as an artifact of numerical calculations.

The back SCSs, characterizing the scattered power into the semi-space above the substrate surface, are shown in Fig. 3. Due to the substrate influence, the back SCSs are reduced at the resonant wavelengths compared to the free space case. For the Si substrate, the back SCS (green solid curve in Fig. 3)

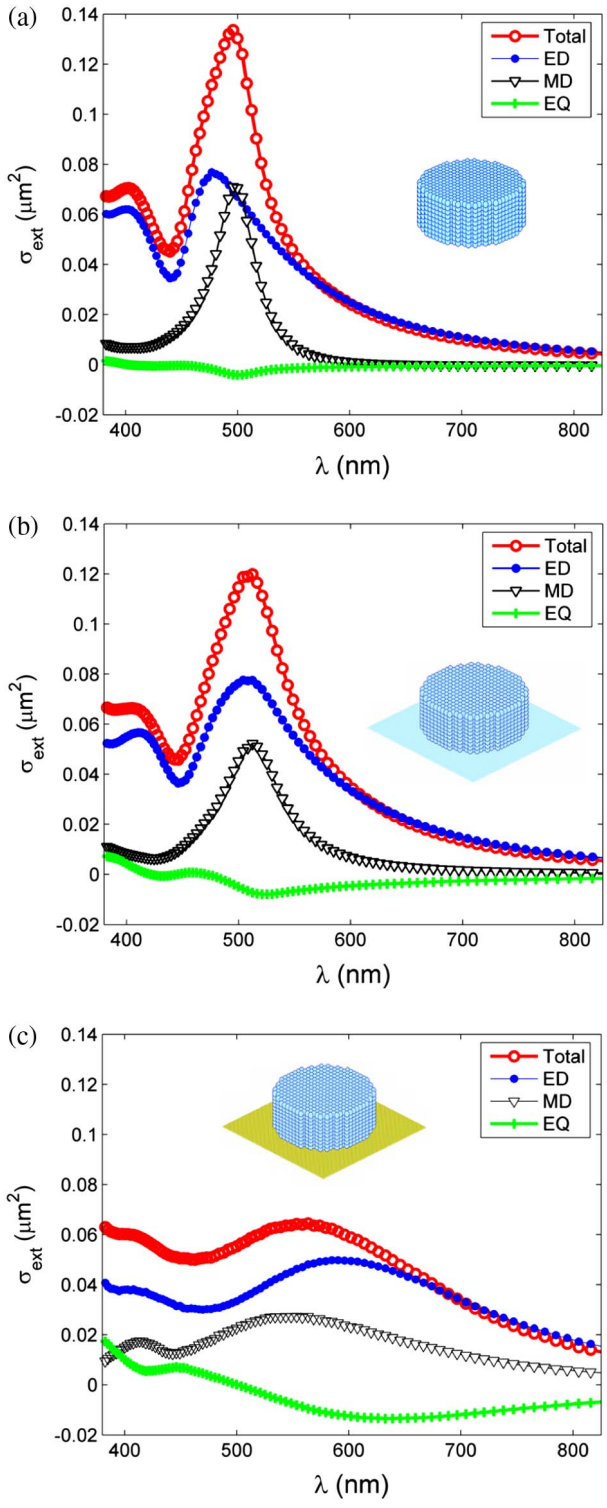

Fig. 2. ECS spectra of cylindrical silicon nanoparticles located (a) in free space, (b) in air on glass substrate, and (c) in air on Si substrate. The particle dimensions are height 75 nm and diameter 150 nm. Normally incident linear-polarized plane waves are considered. Different curves present the total ECS and separate contributions of multipole modes (ED, electric dipole; MD, magnetic dipole; EQ, electric quadrupole).

is small at the resonant wavelength of 560 nm and does not have any peak. So in this case the light scattering occurs in the substrate. This result is in agreement with a recent report

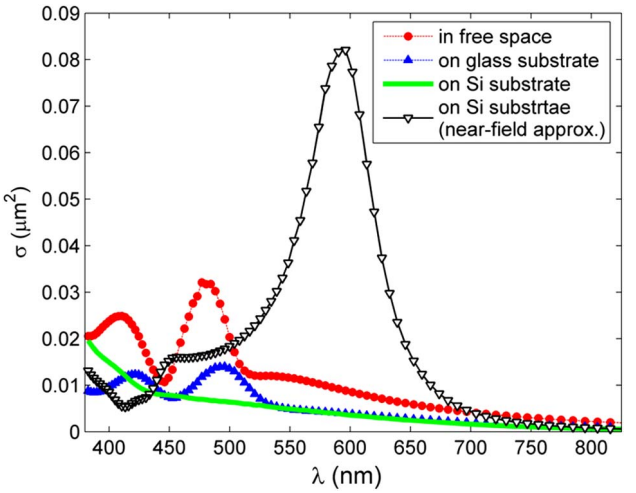

Fig. 3. SCS spectra into the back semi-space (back scattering) for cylindrical Si nanoparticles located in free space, and on glass and Si substrates. The nanoparticle sizes and irradiation conditions are the same as in Fig. 2.

[8], where it was demonstrated that cylindrical Si nanoparticles can effectively couple light into the Si substrate.

In addition to numerical modeling based on the total Green's tensor approach, calculations using the near-field approximation [47] for $\hat{G}_S(\mathbf{r}, \mathbf{r}')$ in Eq. (38) were performed. The result is shown in Fig. 3 (black curve with the resonant peak at $\lambda = 595$ nm). Comparing this curve with the green solid curve, one can see that the near-field approximation provides an incorrect result.

6. CONCLUSIONS

A theoretical approach, allowing the multipole decomposition of extinction and scattering spectra of arbitrary-shaped nanoparticles located in nonhomogeneous environments or near material interfaces, has been demonstrated. The multipole decompositions of the polarization and electric current density induced by external light fields inside an arbitrary-shaped nanoparticle have been presented. The polarization has been calculated numerically using the DDA. In this case, the induced polarization is presented as a finite sum of distributed point electric dipoles with corresponding coordinate delta functions. After the multipole-decomposition procedure, the polarization is transformed into a sum of multipole terms. Inserting this sum into expressions for scattering fields and extinction power, we can obtain their multipole representations. It has been shown how the developed approach can be applied for nanoparticles located on different substrates including substrates supporting propagation of SPPs. Expressions for the fields generated by high-order multipole moments have been obtained. Resonant light scattering by cylindrical Si nanoparticles located on different dielectric substrates has been modeled. It has been shown that interactions between different multipole modes and spectral shifts of optical resonances appear due to the substrate influence. The developed approach can be applied for investigations of radiation generated by different multipole moments located in inhomogeneous environments and for studies of electromagnetic interference effects between the fields generated by different multipoles.

APPENDIX A: MULTIPOLE DECOMPOSITION OF POLARIZATION

Inserting Eq. (4) in Eq. (3), one obtains

$$\mathbf{P}(\mathbf{r}) \simeq \int \mathbf{P}(\mathbf{r}')d\mathbf{r}'\delta(\mathbf{r}-\mathbf{r}_0) - \int \mathbf{P}(\mathbf{r}')(\Delta\mathbf{r}\cdot\nabla)\delta(\mathbf{r}-\mathbf{r}_0)d\mathbf{r}' + \frac{1}{2}\int \mathbf{P}(\mathbf{r}')(\Delta\mathbf{r}\cdot\nabla)^2\delta(\mathbf{r}-\mathbf{r}_0)d\mathbf{r}' + \ldots \quad \text{(A1)}$$

where the integral in the first term of expansion is the dipole moment $\mathbf{p}$. Using the identities $[\mathbf{a}\times[\mathbf{b}\times\mathbf{c}]] = \mathbf{b}(\mathbf{a}\cdot\mathbf{c}) - \mathbf{c}(\mathbf{a}\cdot\mathbf{b})$ and $(\mathbf{ab})\mathbf{c} = \mathbf{a}(\mathbf{b}\cdot\mathbf{c})$, one can write for the second term

$$\mathbf{P}(\Delta\mathbf{r}\cdot\nabla\delta) = \frac{1}{2}(\mathbf{P}\Delta\mathbf{r} + \Delta\mathbf{r}\mathbf{P})\nabla\delta - \frac{1}{2}[\nabla\delta\times[\Delta\mathbf{r}\times\mathbf{P}]], \quad \text{(A2)}$$

where the arguments of $\mathbf{P}$ and δ are omitted. Inserting Eq. (A2) in the second term of Eq. (A1), one can obtain expressions for the electric quadrupole and magnetic dipole terms.

The last term in Eq. (A1) includes the contribution of electric octupole and magnetic quadrupole moments

$$\begin{aligned}\frac{1}{2}\int \mathbf{P}(\mathbf{r}')(\Delta\mathbf{r}\cdot\nabla)^2 d\mathbf{r}'\delta(\mathbf{r}-\mathbf{r}_0) &= \frac{1}{2}\int \mathbf{P}(\mathbf{r}')[(\Delta\mathbf{r}\Delta\mathbf{r}):(\nabla\nabla)\delta(\mathbf{r}-\mathbf{r}_0)]d\mathbf{r}' \\ &= \frac{1}{2}\left[\int \mathbf{P}(\mathbf{r}')\Delta\mathbf{r}\Delta\mathbf{r}d\mathbf{r}'\right]\nabla\nabla\delta(\mathbf{r}-\mathbf{r}_0). \quad \text{(A3)}\end{aligned}$$

Using expression (A10) in [41], we can write

$$P_i\Delta r_j\Delta r_k = -\frac{1}{3}(\Delta r_i\Delta r_j\Delta r_k(\nabla\cdot\mathbf{P}) + \varepsilon_{ijl}[\Delta r\times\mathbf{P}]_l\Delta r_k + \varepsilon_{ikl}[\Delta r\times\mathbf{P}]_l\Delta r_j), \quad \text{(A4)}$$

where ε_{ijk} is the Levi–Civita tensor, where the sum over repeated indexes is assumed. Integrating this expression, we obtain

$$\int P_i\Delta r_j\Delta r_k d\mathbf{r}' = \frac{1}{3}O_{ijk} + \frac{1}{2i\omega}(\varepsilon_{ijl}M_{lk} + \varepsilon_{ikl}M_{lj}), \quad \text{(A5)}$$

where the tensor $\hat{O}$ is the electric octupole moment

$$\hat{O} = -\int \Delta\mathbf{r}\Delta\mathbf{r}\Delta\mathbf{r}(\nabla\cdot\mathbf{P}(\mathbf{r}'))d\mathbf{r}', \quad \text{(A6)}$$

and $\hat{M}$ is the tensor of the magnetic quadrupole moment

$$\hat{M} = -\frac{2i\omega}{3}\int[\Delta\mathbf{r}\times\mathbf{P}(\mathbf{r}')]\Delta\mathbf{r}d\mathbf{r}'. \quad \text{(A7)}$$

Thus,

$$\frac{1}{2}\int \mathbf{P}(\mathbf{r}')(\Delta\mathbf{r}\cdot\nabla)^2 d\mathbf{r}'\delta(\mathbf{r}-\mathbf{r}_0) = \frac{1}{6}\hat{O}(\nabla\nabla\delta(\mathbf{r}-\mathbf{r}_0)) - \frac{i}{2\omega}[\nabla\times\hat{M}\nabla\delta(\mathbf{r}-\mathbf{r}_0)], \quad \text{(A8)}$$

where we used the identity

$$(\varepsilon_{ijl}M_{lk} + \varepsilon_{ikl}M_{lj})(\nabla\nabla\delta(\mathbf{r}-\mathbf{r}_0))_{jk} = 2[\nabla\times\hat{M}\nabla\delta(\mathbf{r}-\mathbf{r}_0)]_i. \quad \text{(A9)}$$

APPENDIX B: ELECTRIC FIELDS RADIATED BY ELECTRIC AND MAGNETIC DIPOLES LOCATED ABOVE A PLANE SURFACE

The angular distribution of electric fields radiated (scattered) into the FF zone by electric and magnetic dipoles located at a point $\mathbf{r}_0 = (x_0, y_0, z_0)$ (Fig. 1) can be easily obtained using spherical coordinate representation, where (r, φ, θ) are the spherical coordinates of the observation point (the Cartesian coordinate system is chosen as shown in Fig. 1) [37].

Above the surface,

(1) the electric field of an electric dipole $\mathbf{p} = (p_x, p_y, p_z)$

$$E^p_\varphi(r,\varphi,\theta) = \frac{k_0^2 e^{ik_d r}}{4\pi\varepsilon_0 r}e^{-ik_d(\mathbf{nr}_0)}(1 + r^{(s)}e^{ik_d 2z_0\cos\theta}) \times (p_y\cos\varphi - p_x\sin\varphi); \quad \text{(B1)}$$

$$E^p_\theta(r,\varphi,\theta) = \frac{k_0^2 e^{ik_d r}}{4\pi\varepsilon_0 r}e^{-ik_d(\mathbf{nr}_0)}([1 - r^{(p)}e^{ik_d 2z_0\cos\theta}] \times (p_x\cos\varphi\cos\theta + p_y\sin\varphi\cos\theta) - p_z\sin\theta[1 + r^{(p)}e^{ik_d 2z_0\cos\theta}]); \quad \text{(B2)}$$

(2) the electric field of a magnetic dipole $\mathbf{m} = (m_x, m_y, m_z)$

$$E^m_\varphi(r,\varphi,\theta) = \sqrt{\frac{\mu_0}{\varepsilon_0}}\frac{k_0 k_d e^{ik_d r}}{4\pi r}e^{-ik_d(\mathbf{nr}_0)} \times ([r^{(s)}e^{ik_d 2z_0\cos\theta} - 1] \times (m_x\cos\varphi\cos\theta + m_y\sin\varphi\cos\theta) + m_z\sin\theta[r^{(s)}e^{ik_d 2z_0\cos\theta} + 1]); \quad \text{(B3)}$$

$$E^m_\theta(r,\varphi,\theta) = \sqrt{\frac{\mu_0}{\varepsilon_0}}\frac{k_0 k_d e^{ik_d r}}{4\pi r}e^{-ik_d(\mathbf{nr}_0)} \times [1 + r^{(p)}e^{ik_d 2z_0\cos\theta}] \times (m_y\cos\varphi - m_x\sin\varphi). \quad \text{(B4)}$$

Here, one should use $\mathbf{n} = (\sin\theta\cos\varphi, \sin\theta\sin\varphi, \cos\theta)$, where φ and θ are the azimuthal and polar angles in the spherical coordinate system, respectively. The reflected electric fields are proportional to the reflection coefficients $r^{(p)}$ and $r^{(s)}$ for p- and s-polarized waves

$$r^{(p)} = \frac{\varepsilon_s\cos\theta - \varepsilon_d\sqrt{\varepsilon_s/\varepsilon_d - \sin^2\theta}}{\varepsilon_s\cos\theta + \varepsilon_d\sqrt{\varepsilon_s/\varepsilon_d - \sin^2\theta}}, \quad \text{(B5)}$$

$$r^{(s)} = \frac{\cos\theta - \sqrt{\varepsilon_s/\varepsilon_d - \sin^2\theta}}{\cos\theta + \sqrt{\varepsilon_s/\varepsilon_d - \sin^2\theta}}. \quad \text{(B6)}$$

Note that the vectors corresponding to electric and magnetic dipoles in the above equations are written in the Cartesian coordinate representations.

On the basis of the above expressions and the rule formulated after Eq. (20), it is easy to derive the spherical coordinate representation of electric fields generated by higher-order multipole moments including magnetic quadrupole and electric octupole moments. For direct waves $\mathbf{N} = -ik_d\mathbf{n}$,

and for reflected waves $\mathbf{N} = -ik_d\tilde{\mathbf{n}}$, where $\tilde{\mathbf{n}} = (\tilde{n}_x, \tilde{n}_y, \tilde{n}_z) = (\sin\theta\cos\varphi, \sin\theta\sin\varphi, -\cos\theta)$. Expressions for the electric field below a surface (in substrate) radiated by an electric dipole can be found in [37].

APPENDIX C: SPP ELECTRIC FIELDS RADIATED BY ELECTRIC AND MAGNETIC DIPOLES

The in-plane distribution of the electric E and magnetic H fields of SPPs radiated (scattered) into the FF zone by the electric and magnetic dipoles located at a point $\mathbf{r}_0 = (x_0, y_0, z_0)$ (the Cartesian coordinate system is chosen as shown in Fig. 1) can be easily obtained in the polar coordinate representation, where (φ, ρ, z) are the polar coordinates of the observation point located above $(z > 0)$ or below $(z < 0)$ the metal substrate.

(1) For an electric dipole located in the medium with ε_d and $z > 0$, we have

$$\begin{aligned} E^{p>}_{\mathrm{SPP}z}(\varphi,\rho,z) &= C\frac{k_0^2}{\varepsilon_0}e^{-ak_pz}\sqrt{\frac{2}{\pi k_p\rho}}e^{i(k_p\rho-\pi/4)} \\ &\quad\times e^{-ik_p(\mathbf{n}'\mathbf{r}_0)}[p_z + ia(p_x\cos\varphi + p_y\sin\varphi)]; \\ E^{p>}_{\mathrm{SPP}\rho}(\varphi,\rho,z) &= -iaE^{p>}_{\mathrm{SPP}z}(\varphi,\rho,z); \\ H^{p>}_{\mathrm{SPP}\varphi}(\varphi,\rho,z) &= -\sqrt{\frac{\varepsilon_0}{\mu_0}}\frac{k_p}{k_0}(1-a^2)E^{p>}_{\mathrm{SPP}z}(\varphi,\rho,z); \end{aligned} \tag{C1}$$

and inside the metal $z < 0$,

$$\begin{aligned} E^{p<}_{\mathrm{SPP}z}(\varphi,\rho,z) &= -a^2e^{(a^2+1)k_pz/a}E^{p>}_{\mathrm{SPP}z}(\varphi,\rho,z) \\ E^{p<}_{\mathrm{SPP}\rho}(\varphi,\rho,z) &= \frac{i}{a}E^{p<}_{\mathrm{SPP}z}(\varphi,\rho,z); \\ H^{p<}_{\mathrm{SPP}\varphi}(\varphi,\rho,z) &= \frac{1}{a^2}\sqrt{\frac{\varepsilon_0}{\mu_0}}\frac{k_p}{k_0}(1-a^2)E^{p<}_{\mathrm{SPP}z}(\varphi,\rho,z), \end{aligned} \tag{C2}$$

where $a = \sqrt{-\varepsilon_d/\varepsilon_s}$, $\cos\varphi = x/\rho$, $\sin\varphi = y/\rho$,

$$C = \frac{iak_p}{2(1-a^2)(1-a^4)}.$$

(2) For an magnetic dipole in the domain $z > 0$,

$$\begin{aligned} E^{m>}_{\mathrm{SPP}z}(\varphi,\rho,z) &= C\sqrt{\frac{\mu_0}{\varepsilon_0}}k_0k_pe^{-ak_pz}\sqrt{\frac{2}{\pi k_p\rho}}e^{i(k_p\rho-\pi/4)} \\ &\quad\times e^{-ik_p(\mathbf{n}'\mathbf{r}_0)}(1-a^2)[m_x\sin\varphi - m_y\cos\varphi]; \\ E^{m>}_{\mathrm{SPP}\rho}(\varphi,\rho,z) &= -iaE^{m>}_{\mathrm{SPP}z}(\varphi,\rho,z); \\ H^{m>}_{\mathrm{SPP}\varphi}(\varphi,\rho,z) &= -\sqrt{\frac{\varepsilon_0}{\mu_0}}\frac{k_p}{k_0}(1-a^2)E^{m>}_{\mathrm{SPP}z}(\varphi,\rho,z); \end{aligned} \tag{C3}$$

in the metal $z < 0$,

$$\begin{aligned} E^{m<}_{\mathrm{SPP}z}(\varphi,\rho,z) &= -a^2e^{(a^2+1)k_pz/a}E^{m>}_{\mathrm{SPP}z}(\varphi,\rho,z) \\ E^{m<}_{\mathrm{SPP}\rho}(\varphi,\rho,z) &= \frac{i}{a}E^{m<}_{\mathrm{SPP}z}(\varphi,\rho,z); \\ H^{m<}_{\mathrm{SPP}\varphi}(\varphi,\rho,z) &= \frac{1}{a^2}\sqrt{\frac{\varepsilon_0}{\mu_0}}\frac{k_p}{k_0}(1-a^2)E^{m<}_{\mathrm{SPP}z}(\varphi,\rho,z). \end{aligned} \tag{C4}$$

Note that the vectors of the electric and magnetic dipoles in the above expressions are taken in the Cartesian coordinate representations and $\mathbf{n}' = \mathbf{n}_p$.

On the basis of these expressions and the rule formulated after Eq. (20), it is easy to derive the polar coordinate representation for the SPP electric and SPP magnetic fields generated by higher-order multipole moments, including magnetic quadrupole and electric octupole moments. One has to take into account that $\mathbf{N} = -ik_p\mathbf{n}_p$, where $\mathbf{n}_p = (\cos\varphi, \sin\varphi, -i\sqrt{-\varepsilon_d/\varepsilon_s})$.

ACKNOWLEDGMENTS

The authors acknowledge financial support of this work by the Schwerpunktprogramm SPP1391, the project CH 179/20-1 of the Deutsche Forschungsgemeinschaft (DFG), and the Laboratory of Nano and Quantum Engineering (LNQE) Hannover. A.B.E. and E.E. are grateful to the Russian Foundation for Basic Research, Grant No. 12-02-00528.

REFERENCES

1. E. Hutter and J. H. Fendler, "Exploitation of localized surface plasmon resonance," Adv. Mater. **16**, 1685–1706 (2004).
2. S. A. Maier, *Plasmonics: Fundamentals and Applications* (Springer, 2007).
3. C. F. Bohren and D. R. Huffman, *Absorption and Scattering of Light by Small Particles* (Wiley, 1983).
4. Q. Zhao, J. Zhou, F. Zhang, and D. Lippens, "Mie resonance based dielectric metamaterial," Mater. Today **12**(12), 60–69 (2009).
5. N. J. Halas, S. Lal, W.-S. Chang, S. Link, and P. Nordlander, "Plasmons in strongly coupled metallic nanostructures," Chem. Rev. **111**, 3913–3961 (2011).
6. V. Giannini, A. I. Fernández-Domnguez, S. C. Heck, and S. A. Maier, "Plasmonic nanoantennas: fundamentals and their use in controlling the radiative properties of nanoemitters," Chem. Rev. **111**, 3888–3912 (2011).
7. A. E. Krasnok, A. E. Miroshnichenko, P. A. Belov, and Y. S. Kivshar, "All-dielectric optical nanoantennas," Opt. Express **20**, 20599–20604 (2012).
8. P. Spinelli, M. A. Verschuuren, and A. Polman, "Broadband omnidirectional antireflection coating based on subwavelength surface Mie resonators," Nat. Commun. **3**, 692 (2012).
9. B. Rolly, B. Stout, and N. Bonod, "Boosting the directivity of optical antennas with magnetic and electric dipolar resonant particles," Opt. Express **20**, 20376–20386 (2012).
10. A. B. Evlyukhin, S. M. Novikov, U. Zywietz, R. L. Eriksen, C. Reinhardt, S. I. Bozhevolnyi, and B. N. Chichkov, "Demonstration of magnetic dipole resonances of dielectric nanospheres in the visible region," Nano Lett. **12**, 3749–3755 (2012).
11. A. I. Kuznetsov, A. E. Miroshnichenko, Y. H. Fu, J. Zhang, and B. Luk'yanchuk, "Magnetic light," Sci. Rep. **2**, 492 (2012).
12. J. Chen, J. Ng, Z. Lin, and C. T. Chan, "Optical pulling force," Nat. Photonics **5**, 531–534 (2011).
13. M. Nieto-Vesperinas, J. J. Sáenz, R. Gómez-Medina, and L. Chantada, "Optical forces on small magnetodielectric particles," Opt. Express **18**, 11428–11443 (2010).
14. A. Ashkin, "Acceleration and trapping of particles by radiation pressure," Phys. Rev. Lett. **24**, 156–159 (1970).
15. D. G. Grier, "A revolution in optical manipulation," Nature **424**, 810–816 (2003).
16. T. Čižmár, L. C. Dávila Romero, K. Dholakia, and D. L. Andrews, "Multiple optical trapping and binding: new routes to self-assembly," J. Phys. B **43**, 102001 (2010).
17. M. L. Juan, M. Righini, and R. Quidant, "Plasmon nano-optical tweezers," Nat. Photonics **5**, 349–356 (2011).
18. E. H. Brandt, "Levitation in physics," Science **243**, 349–355 (1989).

19. L. Shi, E. Xifré-Pérez, F. J. Garca de Abajo, and F. Meseguer, "Looking through the mirror: optical microcavity-mirror image photonic interaction," Opt. Express **20**, 11247–11255 (2012).
20. A. E. Miroshnichenko, S. Flach, and Y. S. Kivshar, "Fano resonances in nanoscale structures," Rev. Mod. Phys. **82**, 2257–2298 (2010).
21. B. Luk'yanchuk, N. I. Zheludev, S. A. Maier, N. J. Halas, P. Nordlander, H. Giessen, and C. T. Chong, "The Fano resonance in plasmonic nanostructures and metamaterials," Nat. Mater. **9**, 707–715 (2010).
22. J. A. Schuller, E. S. Barnard, W. Cai, Y. C. Jun, J. S. White, and M. L. Brongersma, "Plasmonics for extreme light concentration and manipulation," Nat. Mater. **9**, 193–204 (2010).
23. P. Biagioni, J.-S. Huang, and B. Hecht, "Nanoantennas for visible and infrared radiation," Rep. Prog. Phys. **75**, 024402 (2012).
24. M. Abb, Y. Wang, P. Albella, C. H. de Groot, J. Aizpurua, and O. L. Muskens, "Interference, coupling, and nonlinear control of high-order modes in single asymmetric nanoantennas," ASC Nano **6**, 6462–6470 (2012).
25. C. Rockstuhl, C. Menzel, S. Mühlig, J. Petschulat, C. Helgert, C. Etrich, A. Chipouline, T. Pertsch, and F. Lederer, "Scattering properties of metaatoms," Phys. Rev. B **83**, 245119 (2011).
26. C. Menzel, S. Mühlig, C. Rockstuhl, and F. Lederer, "Multipole analysis of meta-atoms," Metamaterials **5**, 64–73 (2011).
27. M. I. Mishchenko, L. D. Travis, and D. W. Mackowski, "*T*-matrix computations of light scattering by nonspherical particles: a review," J. Quant. Spectrosc. Radiat. Transfer **55**, 535–575 (1996).
28. C. Hafner and G. Klaus, "Application of the multiple multipole (MMP) method to electrodynamics," Int. J. Comp. Math. Elect. Electron. Eng. **4**, 137–144 (1985).
29. M. Paulus and O. J. F. Martin, "Light propagation and scattering in stratified media: a Green's tensor approach," J. Opt. Soc. Am. A **18**, 854–861 (2001).
30. E. Eremina, Y. Eremin, and T. Wriedt, "Simulations of light scattering spectra of a nanoshell on plane interface based on the discrete sources method," Opt. Commun. **267**, 524–529 (2006).
31. V. Myroshnychenko, J. Rodrguez-Fernández, I. Pastoriza-Santos, A. M. Funston, C. Novo, P. Mulvaney, L. M. Liz-Marzán, and F. J. Garca de Abajo, "Modelling the optical response of gold nanoparticles," Chem. Soc. Rev. **37**, 1792–1805 (2008).
32. T. T. Søndergaard, "Modeling of plasmonic nanostructures: Green's function integral equation methods," Phys. Status Solidi B **244**, 3448–3462 (2007).
33. A. B. Evlyukhin, C. Reinhardt, and B. N. Chichkov, "Multipole light scattering by nonspherical nanoparticles in the discrete dipole approximation," Phys. Rev. B **84**, 235429 (2011).
34. B. T. Draine, "The discrete-dipole approximation and its application to interstellar graphite grains," Astrophys. J. **333**, 848–872 (1988).
35. B. T. Draine and P. J. Flatau, "Discrete dipole approximation for scattering calculations," J. Opt. Soc. Am. A **11**, 1491–1499 (1994).
36. M. A. Yurkin and A. G. Hoekstra, "The discrete dipole approximation: an overview and recent developments," J. Quant. Spectrosc. Radiat. Transfer **106**, 558–589 (2007).
37. L. Novotny and B. Hecht, *Principles of Nano-Optics* (Cambridge University, 2006).
38. T. Søndergaard and S. I. Bozhevolnyi, "Surface plasmon polariton scattering by a small particle placed near a metal surface: an analytical study," Phys. Rev. B **69**, 045422 (2004).
39. A. B. Evlyukhin, G. Brucoli, L. Martn-Moreno, S. I. Bozhevolnyi, and F. J. Garca-Vidal, "Surface plasmon polariton scattering by finite-size nanoparticles," Phys. Rev. B **76**, 075426 (2007).
40. C. H. Papas, *Theory of Electromagnetic Wave Propagation* (Dover, 1988).
41. R. E. Raab and O. L. de Lange, *Multipole Theory in Electromagnetism* (Clarendon, 2005).
42. P. Mazur and B. R. A. Nijboer, "On the statistical mechanics of matter in an lectromagnetic field. I," Physica **19**, 971–986 (1953).
43. A. B. Evlyukhin, C. Reinhardt, U. Zywietz, and B. N. Chichkov, "Collective resonances in metal nanoparticle arrays with dipole-quadrupole interactions," Phys. Rev. B **85**, 245411 (2012).
44. A. B. Evlyukhin, C. Reinhardt, A. Seidel, B. S. Luk'yanchuk, and B. N. Chichkov, "Optical response features of Si-nanoparticle arrays," Phys. Rev. B **82**, 045404 (2010).
45. L. Novotny, B. Hecht, and D. W. Pohl, "Interference of locally excited surface plasmons," J. Appl. Phys. **81**, 1798–1806 (1997).
46. M. Paulus, P. Gay-Balmaz, and O. J. F. Martin, "Accurate and efficient computation of the Green's tensor for stratified media," Phys. Rev. E **62**, 5797–5807 (2000).
47. Z. Li, B. Gu, and G. Yang, "Modified self-consistent approach applied in near-field optics for mesoscopic surface defects," Phys. Rev. B **55**, 10883–10894 (1997).
48. E. Palik, *Handbook of Optical Constant of Solids* (Academic, 1985).
49. G. Gantzounis, "Plasmon modes of axisymmetric metallic nanoparticles: a group theory analysis," J. Phys. Chem. C **113** 21560–21565 (2009).
50. M. W. Knight, Y. Wu, J. B. Lassiter, P. Nordlander, and N. J. Halas, "Substrates matter: influence of an adjacent dielectric on an individual plasmonic nanoparticle," Nano Lett. **9**, 2188–2192 (2009).
51. S. Zhang, K. Bao, N. J. Halas, H. Xu, and P. Nordlander, "Substrate-induced Fano resonances of a plasmonic nanocube: a route to increased-sensitivity localized surface plasmon resonance sensors revealed," Nano Lett. **11**, 1657–1663 (2011).